Commun. Comput. Phys.
doi: 10.4208/cicp.030709.161209a

Vol. **8**, No. 4, pp. 877-900
October 2010

A Node-Centered Artificial Viscosity Method for Two-Dimensional Lagrangian Hydrodynamics Calculations on a Staggered Grid

A. Burbeau-Augoula*

CEA, DIF, F-91297 Arpajon, France.

Received 3 July 2009; Accepted (in revised version) 16 December 2009

Communicated by Chi-Wang Shu

Available online 17 May 2010

Abstract. This work deals with the simulation of two-dimensional Lagrangian hydrodynamics problems. Our objective is the development of an artificial viscosity that is to be used in conjunction with a staggered placement of variables: thermodynamics variables are centered within cells and position and fluid velocity at vertices. In [J. Comput. Phys., 228 (2009), 2391-2425], Maire develops a high-order cell-centered scheme for solving the gas dynamics equations. The numerical results show the accuracy and the robustness of the method, and the fact that very few Hourglass-type deformations are present. Our objective is to establish the link between the scheme of Maire and the introduction of artificial viscosity in a Lagrangian code based on a staggered grid. Our idea is to add an extra degree of freedom to the numerical scheme, which is an approximation of the fluid velocity within cells. Doing that, we can locally come down to a cell-centered approximation and define the Riemann problem associated to discrete variable discontinuities in a very natural way. This results in a node-centered artificial viscosity formulation. Numerical experiments show the robustness and the accuracy of the method, which is very easy to implement.

AMS subject classifications: 65M08, 76E06, 65Z05, 80M12

Key words: Hydrodynamics, staggered discretization, artificial viscosity, Lagrangian simulation, shock waves, finite volume scheme.

1 Introduction

In the context of multimaterial flows modeling, calculations are traditionally carried out using Lagrangian numerical methods which are accurate and well tested for tracking material properties. In this paper, we are interested in Lagrangian numerical based codes for

*Corresponding author. *Email address:* anne.burbeau-augoula@cea.fr (A. Burbeau-Augoula)

the simulation of two dimensional hydrodynamics problems. A possible method to treat these problems is to consider a staggered localization of variables: thermodynamics variables are centered within cells and position and fluid velocity are at vertices. This allows the mesh to be trivially moved with the fluid velocity. Basic principles and difficulties in the discretization of the equations of fluid dynamics written in Lagrangian form can be found in [20]. More recently, Caramana et al. [4] showed how to construct compatible hydrodynamics algorithms. The problem of the elimination of Hourglass-type motions and artificial grid distortions is investigated in [21]. In the presence of solution discontinuities, a special treatment is necessary to model shock waves. It is usual to introduce an artificial viscosity term to smear out numerical shock profiles over a number of zones to reduce post-shock oscillations. The pioneering method is due to Von Neumann and Richtmyer and concerns one- dimensional flows [1]. They introduce an explicit artificial viscosity term to smear a shock discontinuity in space without affecting the Hugoniot conditions across the shock. The viscous stress is represented by a scalar pressure of the form

$$q=-\rho|\Delta u|\Delta u.$$

This term is quadratic in Δu, where Δu is the velocity jump across the element. The work done by the viscosity is identified with the thermodynamic irreversibility of the shock. Von Neumann and Richtmyer are at the origin of all the progress that occurred on the design of artificial viscosity afterwards. Landshoff notices in [15] that with a quadratic viscosity formulation, small oscillations still occur after the shock. He proposes a linear combination of a linear and a quadratic viscosities

$$q=C_1\rho(\Delta u)^2+C_2a\rho|\Delta u|,$$

where a is the local sound speed and C_1 and C_2 are non-dimensional constants. In [8], Wilkins recalls that Kurapatenko has established another form of the viscosity term from the pressure jump across a shock in an ideal gas. By considering the limit of Kurapatenko's solution when the velocity jump tends to zero, a linear viscosity is obtained. The formulation reduces to a quadratic term as Δu becomes large. This provides a supplementary justification of the formulation proposed by Landshoff [15].

The generalization of the method for multidimensional flows raises many difficulties. The first one is concerned with the determination of the tensor character of the viscosity due to the velocity gradient. Then, one has to choose an approximation of the shock direction and a length scale. This last one has a non negligible effect on the computation robustness when quadrilateral cells have very different sizes for adjacent edges (typically large aspect ratio), which occurs very frequently in Lagrangian simulations. The simplest extension of the viscosity from one to two dimensions is to consider a viscosity as a pressure term. We have to compute a velocity jump across the shock in the element. Numerical results are strongly dependent on the approximation of the shock direction. The work associated to the viscosity term is treated as a pressure (the viscosity has the same effect in all the directions), which results in shock overheating. In [2], Schulz generalizes the scalar artificial viscosity into a tensor artificial viscosity in 2D. He develops a

method in which the artificial viscosity is computed at cell edges rather than cell centers. By this way, the viscosity has no effect along a wave of constant phase. More recently, Caramana et al. [3] published a very complete paper devoted to the presentation of an edge-centered viscosity based on Schulz's ideas [2]. Authors propose a set of criteria that any artificial viscosity should satisfy. The paper reverts to some fundamentals and many references are given. In this work, Caramana et al. end at the development of the most efficient edge-centered viscosity. The edge-centered methods work reasonably well, but they suffer from the appearance of a non physical vorticity in particular cases. Let's consider the Noh problem [16] with Lagrangian grid not aligned with the flow (for example the spherical Noh problem with an initially square grid). Jets are formed along the axis which result in a highly deformed mesh. This problem is analyzed by Campbell and Shashkov in [13]. In their opinion, "the reason for this is that the edge viscosity does not model physical viscosity and therefore does not have a well defined continuum limit". Campbell and Shashkov propose a method based on an approximation to a quantity which may be related to physical viscosity and has a tensor nature. The results for the spherical Noh problem on a Cartesian mesh are very good. The spherical symmetry of the flow is well preserved. For a review of viscosity formulations, the reader can refer to [20] and the references proposed in [3]. Up to now, we have mentioned methods for shock capturing all based on the introduction of an explicit viscosity term into the equations. A radically different method, applied in an Eulerian context and introduced by Godunov [7] has to be cited. It consists of considering all quantities in a computational cell to be constant at the start of a time step and to resolve the resultant discontinuities at the cell edges by the solution of a Riemann problem. The advantage of this method is that it does not require the addition of an explicit artificial viscosity. Numerical diffusion is added implicitly in the Riemann solution in a very natural way. The two approaches for the capture of shock waves (either by adding an explicit artificial viscosity force or by using approximate Riemann solvers) are similar [5, 6]. It just so happens that in the context of Lagrangian codes based on staggered grids, shocks are principally treated with artificial viscosity.

We propose here an alternative view point to introduce artificial viscosity in a code based on a staggered mesh. This work is motivated by recent progress in the design of cell-centered schemes for equations of gas dynamics written in a Lagrangian formalism [10–12, 14]. A node-based discretization of the numerical fluxes has been developed. The extensive numerical results presented by Maire et al. [10–12] show very few "Hourglassing modes" in comparison with our past experience. Their scheme is very robust and accurate. Despite the fact that the Finite Volume scheme proposed by Maire et al. is based on a centered placement of variables, it seems to be very close to that of Wilkins. We established the link between the scheme of Maire et al. [10] and a finite volume scheme based on a staggered grid with artificial viscosity. As a result, we propose a new formulation for artificial viscosity. The principal interests of this work are:

• the simplicity of the method which can be easily implemented in an existing code based on a staggered grid (in the context of codes based on multi-physics modelling, the

modification of the hydro scheme can raise many difficulties);

• its original construction which could participate in a better understanding of the difficulties encountered in Lagrangian simulations (production of non-physical vorticity, presence of "Hourglass-type" deformations,$\cdots$,);

• the robustness and the accuracy of the algorithm are entirely reasonable.

In Section 2, Lagrangian hydrodynamics equations are presented. Section 3 is devoted to the presentation of the spatial discretization of the equations in the absence of shock waves. Then, in Section 4, the problem of shock capturing is treated. In Section 5, numerical experiments are proposed.

2 Equations of Lagrangian hydrodynamics

Let $\Omega(t)$ be a moving control volume. We denote by ρ the mass density, $\overrightarrow{u}=(u,v)^t$ the fluid velocity, P the pressure, E the specific total energy and ϵ the specific internal energy of the fluid. We consider the conservation equations of mass, momentum, total energy and volume in the Lagrangian formalism ($\mathrm{d}/\mathrm{d}t$ is the total time derivative following the fluid element)

$$\frac{\mathrm{d}}{\mathrm{d}t}\int_{\Omega(t)}\rho\,\mathrm{d}v=0, \tag{2.1}$$

$$\frac{\mathrm{d}}{\mathrm{d}t}\int_{\Omega(t)}\rho\overrightarrow{u}\,\mathrm{d}v+\int_{\Omega(t)}\overrightarrow{\nabla}P\,\mathrm{d}v=0, \tag{2.2}$$

$$\frac{\mathrm{d}}{\mathrm{d}t}\int_{\Omega(t)}\rho E\,\mathrm{d}v+\int_{\Omega(t)}\overrightarrow{\nabla}\cdot\left(P\overrightarrow{u}\right)\,\mathrm{d}v=0, \tag{2.3}$$

$$\frac{\mathrm{d}}{\mathrm{d}t}\int_{\Omega(t)}\mathrm{d}v=\int_{\Omega(t)}\overrightarrow{\nabla}\cdot\overrightarrow{u}\,\mathrm{d}v. \tag{2.4}$$

Eq. (2.4) is named Geometric Conservation Law (GCL). It states that the velocity displacement of a moving control volume is locally equal to the fluid velocity. The discretization of this equation is a key point in the construction of a purely Lagrangian scheme, the difficulty being to ensure consistency with the GCL discretization.

In the absence of shock waves, the equation for the total energy can be replaced by an equation on the internal energy

$$\frac{\mathrm{d}}{\mathrm{d}t}\int_{\Omega(t)}\rho\epsilon\,\mathrm{d}v+\int_{\Omega(t)}P\overrightarrow{\nabla}\cdot\overrightarrow{u}\,\mathrm{d}v=0. \tag{2.5}$$

3 Spatial discretization

In this section, some useful notations are introduced. Then, the spatial discretization is briefly recalled.

3.1 Notations

We consider an unstructured grid made of quadrangular elements. A cell Q is defined by points j. The median mesh is formed by connecting the cell centers to the mid-side points of edges surrounding node j. The dual cell associated to node j is denoted by $\mathcal{C}_j$ (see Fig. 1).

The following notations will be used throughout the paper.

• The notation j (resp. Q) always refers to a node (resp. a cell);

• $\sum_Q$ denotes the sum over **all the mesh cells**; $\sum_j$ denotes the sum over **all the mesh nodes**; $\sum_{Q,Q\ni j}$ denotes the sum over **cells** Q **surrounding node** j; $\sum_{j,j\in Q}$ denotes the sum over **nodes** j **of cell** Q; $\bigcup_{Q,Q\ni j}$ denotes the set of **cells** Q **that share point** j; $\bigcup_{j,j\in Q}$ denotes the set of **vertices** j **of cell** Q;

• The corner volume $\mathcal{C}_{Q,j}$ is associated with the grid point j and the cell Q: it is defined by the volume inside the surface defined through the point j, the center point of cell Q and the midpoints of the edges through point j of cell Q (see Fig. 1). It follows that

$$\mathcal{C}_j=\bigcup_{Q,Q\ni j}\mathcal{C}_{Q,j},\quad \bigcup_{j,j\in Q}\mathcal{C}_{Q,j}=Q;$$

• A **subscript is used to indicate if the variable is associated to (or computed at) a node, a cell or an edge**. For example, f_j is the approximate value of function f at node j. If there is a possible ambiguity, or if further precise details are necessary, a **superscript** is used. For example, f_j^Q is the discrete value of function f at the node point j, associated to cell Q;

• The point associated to node j is denoted by M_j;

• Consider the point M_j. This point belongs to a cell Q. The nodes of the cell are now locally numbered anti-clockwise. The node j corresponds to the point M_j, and we introduce the nodes $j\pm1$ which correspond to the points $M_{j\pm1}^Q$ represented on Fig. 2. $M_{j+1/2}^Q$ (resp. $M_{j-1/2}^Q$) is the midpoint of edge $[M_j^Q,M_{j+1}^Q]$ (resp. $[M_{j-1}^Q,M_j^Q]$) of cell Q;

• Consider a cell Q. The subscript $e(j,j+1)$ is used for a variable associated to the **edge** $[M_j^Q,M_{j+1}^Q]$. Thus, $f_{e(j,j+1)}^Q$ is the discrete value of function f associated to the edge $e(j,j+1)$ of cell Q;

• According to this convention, $\overrightarrow{n}_{e(j,j+1)}^Q$ (resp. $\overrightarrow{n}_{e(j-1,j)}^Q$) is the outward unit normal vector of edge $[M_j^Q,M_{j+1}^Q]$ (resp. $[M_{j-1}^Q,M_j^Q]$) of cell Q;

• The subscript $(e/2)(j,j+1/2)$ is used for a variable associated to the **half-edge** $[M_j^Q,M_{j+1/2}^Q]$. Thus, $f_{\frac{1}{2}e(j,j+1/2)}^Q$ is the discrete value of function f associated to the half-edge $(e/2)(j,j+1/2)$ of cell Q;

• The length of the half-edge$[M_j^Q,M_{j+1/2}^Q]$ (resp. $[M_{j-1/2}^Q,M_j^Q]$) is $L_{\frac{1}{2}e(j,j+1/2)}^Q$ (resp. $L_{\frac{1}{2}e(j-1/2,j)}^Q$).

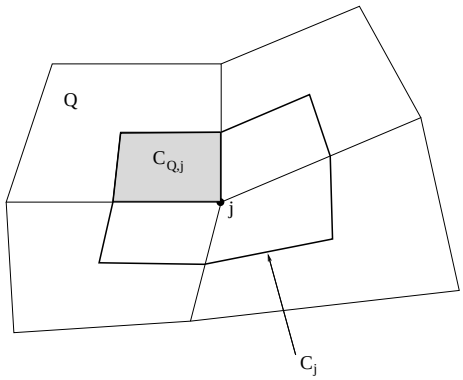

Figure 1: Grid with respect to cell Q and point j.

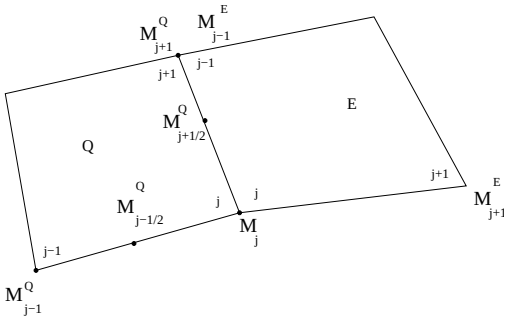

Figure 2: Notations with respect to the mesh point M_j, shared by two cells Q and E.

3.2 Numerical scheme

We consider Cartesian (X,Y) coordinates (the case of cylindrical coordinates with symmetry about an axis is discussed in Section 4.5). The conservation equations for mass, momentum and internal energy are semi-discretized in space using a finite volume scheme on a staggered grid [9]. The position and velocity are defined at grid points and density, internal energy and the pressure are defined at cell centers.

We introduce

$$\rho_Q \simeq \frac{\int_Q \rho \, \mathrm{d}X\mathrm{d}Y}{\int_Q \mathrm{d}X\mathrm{d}Y}, \qquad \overrightarrow{u}_j \simeq \frac{\int_{\mathcal{C}_j} \rho \overrightarrow{u} \, \mathrm{d}X\mathrm{d}Y}{\int_{\mathcal{C}_j} \rho \, \mathrm{d}X\mathrm{d}Y},$$

$$\epsilon_Q \simeq \frac{\int_Q \rho\epsilon \, \mathrm{d}X\mathrm{d}Y}{\int_Q \rho \, \mathrm{d}X\mathrm{d}Y}, \qquad V_Q = \int_Q \mathrm{d}X\mathrm{d}Y.$$

The approximation of the pressure on cell Q is denoted by P_Q.

We define the element mass

$$m_Q = \rho_Q V_Q. \tag{3.1}$$

Eq. (2.1) is integrated on cell Q to give

$$\frac{\mathrm{d}}{\mathrm{d}t}m_Q=0. \tag{3.2}$$

In practice, the volume of the cell is updated at each time iteration with its node coordinates. Then, the density is computed using Eq. (3.1).

If we consider the equation of continuity for the cell density $\big($with ρ_Q defined as $\rho_Q(t)=m_Q/V_Q(t)\big)$, one obtains a definition of the discrete divergence operator

$$\frac{1}{V_Q}\frac{\mathrm{d}V_Q}{\mathrm{d}t}=(\overrightarrow{\nabla}\cdot\overrightarrow{u})_Q. \tag{3.3}$$

This equation is used for the internal energy equation discretization. The fluid velocity being computed on nodes j, equation for momentum conservation (2.2) is integrated on the dual mesh elements

$$\frac{\mathrm{d}}{\mathrm{d}t}\int_{\mathcal{C}_j}\rho\,\overrightarrow{u}\;\mathrm{d}X\mathrm{d}Y+\int_{\mathcal{C}_j}\overrightarrow{\nabla}P\;\mathrm{d}X\mathrm{d}Y=0. \tag{3.4}$$

We introduce the nodal mass

$$m_j=\int_{\mathcal{C}_j}\rho\;\mathrm{d}X\mathrm{d}Y, \tag{3.5}$$

and by supposing that the nodal mass is Lagrangian, we get

$$m_j\frac{\mathrm{d}\overrightarrow{u}_j}{\mathrm{d}t}+\sum_{Q,Q\ni j}P_Q\int_{(\partial\mathcal{C}_j)\cap Q}\overrightarrow{n}\;\mathrm{d}S=0. \tag{3.6}$$

Equation for internal energy (2.5) is integrated on each cell Q

$$m_Q\frac{\mathrm{d}\epsilon_Q}{\mathrm{d}t}+P_Q\int_Q\overrightarrow{\nabla}\cdot\overrightarrow{u}\;\mathrm{d}X\mathrm{d}Y=0. \tag{3.7}$$

Using Eq. (3.3), the divergence operator is chosen consistent with the mesh displacement

$$m_Q\frac{\mathrm{d}\epsilon_Q}{\mathrm{d}t}+P_Q\frac{\mathrm{d}V_Q(t)}{\mathrm{d}t}=0. \tag{3.8}$$

This scheme in its semi-discrete form satisfies a local entropy equality. Indeed, the time rate of change of the specific entropy S_Q in cell Q is

$$m_QT_Q\frac{\mathrm{d}S_Q}{\mathrm{d}t}=m_Q\frac{\mathrm{d}\epsilon_Q}{\mathrm{d}t}+P_Q\frac{\mathrm{d}V_Q}{\mathrm{d}t}, \tag{3.9}$$

and from Eq. (3.8), we get

$$m_QT_Q\frac{\mathrm{d}S_Q}{\mathrm{d}t}=0. \tag{3.10}$$

This equality has to be replaced by an inequality of the form

$$m_Q T_Q \frac{\mathrm{d}S_Q}{\mathrm{d}t} > 0,$$

in the presence of shock waves. This is precisely the goal of artificial viscosity that converts kinetic energy into internal energy consistently with the second law of thermodynamics.

4 Artificial viscosity

The definition of the viscosity term in the case of a staggered placement of variables is a difficult task. Indeed, the definition of the Riemann problem (at the origin of any artificial viscosity method, whereas it is not always clearly mentioned) is not trivial.

To get round this difficulty, we suppose the approximation of both thermodynamics and velocity variables are cell-centered. The definition of the cell-velocity is established in the construction of the artificial viscosity.

4.1 Presentation of a node-based viscosity method

We use the sub-cell forces formalism first introduced in the framework of staggered Lagrangian scheme [4] and used by Maire [11] in the elaboration of its cell-centered Lagrangian scheme. Eq. (3.6) is re-written as

$$m_j \frac{\mathrm{d}\overrightarrow{u}_j}{\mathrm{d}t} = \overrightarrow{f}_j^{\mathrm{pres}} = \sum_{Q, Q \ni j} (\overrightarrow{f}_j^{Q})^{\mathrm{pres}}, \tag{4.1}$$

with

$$\begin{aligned}(\overrightarrow{f}_j^{Q})^{\mathrm{pres}} &= -P_Q \int_{(\partial \mathcal{C}_j) \cap Q} \overrightarrow{n}\, \mathrm{d}S = P_Q \int_{\mathcal{C}_j \cap (\partial Q)} \overrightarrow{n}\, \mathrm{d}S \\ &= P_Q \Big(\overrightarrow{n}^{Q}_{e(j-1,j)} L^{Q}_{\frac{1}{2}e(j-1/2,j)} + \overrightarrow{n}^{Q}_{e(j,j+1)} L^{Q}_{\frac{1}{2}e(j,j+1/2)} \Big),\end{aligned} \tag{4.2}$$

where we apply the trivial relation

$$\int_{(\partial \mathcal{C}_j) \cap Q} \overrightarrow{n}\, \mathrm{d}S + \int_{\mathcal{C}_j \cap (\partial Q)} \overrightarrow{n}\, \mathrm{d}S = 0. \tag{4.3}$$

By noting that [23]

$$\frac{\mathrm{d}V_Q}{\mathrm{d}t} = \sum_{j, j \in Q} \overrightarrow{u}_j \cdot \Big(\overrightarrow{n}^{Q}_{e(j-1,j)} L^{Q}_{\frac{1}{2}e(j-1/2,j)} + \overrightarrow{n}^{Q}_{e(j,j+1)} L^{Q}_{\frac{1}{2}e(j,j+1/2)} \Big), \tag{4.4}$$

Eq. (3.8) becomes

$$m_Q \frac{\mathrm{d}\epsilon_Q}{\mathrm{d}t} = -\sum_{j,j\in Q} \overrightarrow{u}_j \cdot \left(\overrightarrow{f}_j^{\,Q}\right)^{\mathrm{pres}}. \tag{4.5}$$

Our objective now is to build a viscous force that is introduced in the equations as follows:

$$m_j \frac{\mathrm{d}\overrightarrow{u}_j}{\mathrm{d}t} = \overrightarrow{f}_j^{\,\mathrm{pres}} + \overrightarrow{f}_j^{\,\mathrm{visc}}, \qquad \overrightarrow{f}_j^{\,\mathrm{visc}} = \sum_{Q,Q\ni j} \left(\overrightarrow{f}_j^{\,Q}\right)^{\mathrm{visc}}, \tag{4.6a}$$

$$m_Q \frac{\mathrm{d}\epsilon_Q}{\mathrm{d}t} = -\sum_{j,j\in Q} \overrightarrow{u}_j \cdot \left(\left(\overrightarrow{f}_j^{\,Q}\right)^{\mathrm{pres}} + \left(\overrightarrow{f}_j^{\,Q}\right)^{\mathrm{visc}} \right). \tag{4.6b}$$

We proceed like in the framework of the cell-centered finite volume scheme of Maire et al. [10, 11]: on the half-edge $[M_j^Q, M_{j+1/2}^Q]$ (resp. $[M_{j-1/2}^Q, M_j^Q]$), we introduce a pressure term $\Pi^Q_{\frac{1}{2}e(j,j+1/2)}$ (resp. $\Pi^Q_{\frac{1}{2}e(j-1/2,j)}$). These half-pressures are considered in the place of the cell pressure in the momentum equation to give

$$m_j \frac{\mathrm{d}\overrightarrow{u}_j}{\mathrm{d}t} = \sum_{Q,Q\ni j} \left(\Pi^Q_{\frac{1}{2}e(j-1/2,j)} \overrightarrow{n}^{\,Q}_{e(j-1,j)} L^Q_{\frac{1}{2}e(j-1/2,j)} + \Pi^Q_{\frac{1}{2}e(j,j+1/2)} \overrightarrow{n}^{\,Q}_{e(j,j+1)} L^Q_{\frac{1}{2}e(j,j+1/2)} \right), \tag{4.7}$$

and then

$$\begin{aligned} \left(\overrightarrow{f}_j^{\,Q}\right)^{\mathrm{visc}} = & \left(\Pi^Q_{\frac{1}{2}e(j-1/2,j)} - P_Q\right) \overrightarrow{n}^{\,Q}_{e(j-1,j)} L^Q_{\frac{1}{2}e(j-1/2,j)} \\ & + \left(\Pi^Q_{\frac{1}{2}e(j,j+1/2)} - P_Q\right) \overrightarrow{n}^{\,Q}_{e(j,j+1)} L^Q_{\frac{1}{2}e(j,j+1/2)}. \end{aligned} \tag{4.8}$$

We see that the method depends only on the definition of the scalar terms associated to each half-edge.

At this point, we slightly modify the discrete problem to be solved. We began the method by considering a staggered grid formulation with momentum defined at the nodes and density and energy in the cells. Now, we introduce an extra degree of freedom $\overrightarrow{u}^{\star}_Q$ and **we suppose it is an approximate fluid velocity within element** Q. To summarize:

• We compute a piecewise constant approximation of the whole solution $(\rho, \overrightarrow{u}, P)$ on each element Q:

$$\rho_Q, \ \overrightarrow{u}^{\star}_Q, \ \epsilon_Q,$$

- the cell density ρ_Q is obtained from Eq. (3.2);
- the internal energy ϵ_Q is given by the resolution of the second equation of (4.6). Of course, the viscous force has to be fully defined first;
- the method for the computation of $\overrightarrow{u}^{\star}_Q$ has not been established yet.

• We compute a piecewise constant approximate solution of the fluid velocity on the dual cell associated to node j, $\overrightarrow{u}_j$, by solving momentum evolution equation (4.7).

The next step in our derivation of the method is the specification of the half-edge pressure terms.

One natural way to proceed consists in solving two half-Riemann problems on each cell edge. First, on the half edge $[M_j^Q, M_{j+1/2}^Q]$ (the arguments are the same for any half edge), we can suppose the velocity is equal to the point velocity $\overrightarrow{u}_j$. Second, on element Q, we also consider $\overrightarrow{u}_Q^\star$ as an approximation of the fluid velocity. Consequently, the one-dimensional problem is defined by the discontinuity of the fluid velocity on the cell boundary ($\overrightarrow{u}_j \cdot \overrightarrow{n}^Q_{e(j,j+1)}$ and $\overrightarrow{u}_Q^\star \cdot \overrightarrow{n}^Q_{e(j,j+1)}$), with two states that are uniform vs ρ and P ($\rho = \rho_Q$ and $P = P_Q$) (see Fig. 3).

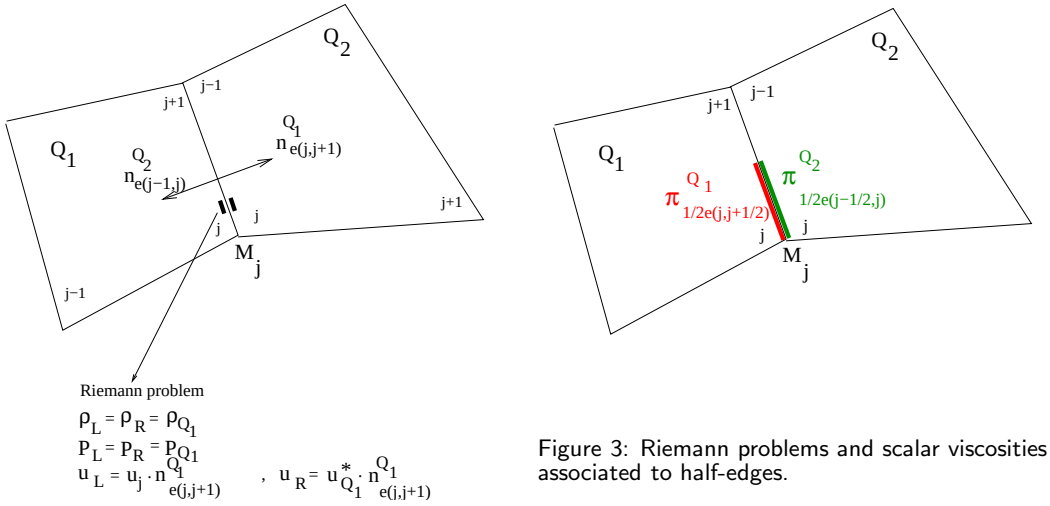

Figure 3: Riemann problems and scalar viscosities associated to half-edges.

This problem is approximately solved using the HLL Riemann solver [5] that gives the expression for the pressure jump across the solution discontinuity:

$$P_Q - \Pi^Q_{\frac{1}{2}e(j,j+1/2)} = -\mu^Q_{\frac{1}{2}e(j,j+1/2)} (\overrightarrow{u}_Q^\star - \overrightarrow{u}_j) \cdot \overrightarrow{n}^Q_{e(j,j+1)}, \tag{4.9a}$$

$$P_Q - \Pi^Q_{\frac{1}{2}e(j-1/2,j)} = -\mu^Q_{\frac{1}{2}e(j-1/2,j)} (\overrightarrow{u}_Q^\star - \overrightarrow{u}_j) \cdot \overrightarrow{n}^Q_{e(j-1,j)}. \tag{4.9b}$$

The coefficients $\mu^Q_{\frac{1}{2}e(j,j+1/2)}$ and $\mu^Q_{\frac{1}{2}e(j-1/2,j)}$ are determined following the approach suggested by Dukowicz [5] and considered by Maire [11]:

$$\mu^Q_{\frac{1}{2}e(j,j+1/2)} = \rho_Q \left(\alpha \left| (\overrightarrow{u}_Q^\star - \overrightarrow{u}_j) \cdot \overrightarrow{n}^Q_{e(j,j+1)} \right| + a_Q \right), \tag{4.10a}$$

$$\mu^Q_{\frac{1}{2}e(j-1/2,1)} = \rho_Q \left(\alpha \left| (\overrightarrow{u}_Q^\star - \overrightarrow{u}_j) \cdot \overrightarrow{n}^Q_{e(j-1,j)} \right| + a_Q \right). \tag{4.10b}$$

In (4.9), a_Q is the local isentropic speed of sound and α is a material dependent quantity which can be derived from the equation of state. $\overrightarrow{u}^{\star}_{Q}$ is still unknown and will be determined later.

A matrix formalism can be introduced to obtain a generic expression for the viscous force. By setting

$$\mathcal{M}^{Q}_{j}=\mathcal{M}^{Q}_{\frac{1}{2}e(j-1/2,j)}+\mathcal{M}^{Q}_{\frac{1}{2}e(j,j+1/2)}, \tag{4.11}$$

with

$$\mathcal{M}^{Q}_{\frac{1}{2}e(j-1/2,j)}=\mu^{Q}_{\frac{1}{2}e(j-1/2,j)}\,\overrightarrow{n}^{Q}_{e(j-1,j)}\otimes\overrightarrow{n}^{Q}_{e(j-1,j)}L^{Q}_{\frac{1}{2}e(j-1/2,j)}, \tag{4.12a}$$

$$\mathcal{M}^{Q}_{\frac{1}{2}e(j,j+1/2)}=\mu^{Q}_{\frac{1}{2}e(j,j+1/2)}\,\overrightarrow{n}^{Q}_{e(j,j+1)}\otimes\overrightarrow{n}^{Q}_{e(j,j+1)}L^{Q}_{\frac{1}{2}e(j,j+1/2)}, \tag{4.12b}$$

we get

$$(\overrightarrow{f}^{Q}_{j})^{\text{visc}}=\mathcal{M}^{Q}_{j}(\overrightarrow{u}^{\star}_{Q}-\overrightarrow{u}_{j}). \tag{4.13}$$

As expected, this expression is similar to the constitutive relation established by Maire [11] in the construction of the viscous sub-cell force for its cell-centered scheme. This equation links the cell velocities and the node velocities. In the case of a linear solver ($\alpha=0$) the matrix $\mathcal{M}^{Q}_{j}$ only contains geometrical information. The following important problems arise:

1. The half-edge pressures are discontinuous through the edge (see Fig. 3). How to ensure momentum and energy conservations?

2. Does the scheme satisfy an entropy inequality?

3. How to compute the velocities $\overrightarrow{u}^{\star}_{Q}$?

All these problems are solved from the same argument: an entropy inequality immediately follows from the derivation of sufficient conditions for the scheme to be conservative [11,14]. These conditions are precisely imposed in the computation of the element velocity $\overrightarrow{u}^{\star}_{Q}$.

First, we establish a sufficient condition to get conservation properties. Momentum is conserved if (by supposing the nodal mass is Lagrangian)

$$\frac{\mathrm{d}}{\mathrm{d}t}\Big(\sum_{j}m_j\overrightarrow{u}_j\Big)=\sum_{j}\big(\overrightarrow{f}^{\text{pres}}_{j}+\overrightarrow{f}^{\text{visc}}_{j}\big)=0. \tag{4.14}$$

Since the pressure forces are computed with respect to the median mesh of the staggered spatial grid discretization, it is trivial to check that

$$\sum_{j}\overrightarrow{f}^{\text{pres}}_{j}=\overrightarrow{0}.$$

Indeed,

$$\sum_{j}\overrightarrow{f}^{\text{pres}}_{j}=\sum_{j}\Big(\sum_{Q,Q\ni j}(\overrightarrow{f}^{Q}_{j})^{\text{pres}}\Big)=\sum_{Q}\Big(\sum_{j,j\in Q}(\overrightarrow{f}^{Q}_{j})^{\text{pres}}\Big),$$

and on each cell Q, we have

$$\sum_{j,j\in Q}(\overrightarrow{f}_j^Q)^{\text{pres}}=P_Q\sum_{j,j\in Q}\Big(\overrightarrow{n}^Q_{e(j-1,j)}L^Q_{\frac{1}{2}e(j-1/2,j)}+\overrightarrow{n}^Q_{e(j,j+1)}L^Q_{\frac{1}{2}e(j,j+1/2)}\Big)=0.$$

In the same way, for the viscous forces we have

$$\sum_j\overrightarrow{f}_j^{\text{visc}}=\sum_j\Big(\sum_{Q,Q\ni j}(\overrightarrow{f}_j^Q)^{\text{visc}}\Big)=\sum_Q\Big(\sum_{j,j\in Q}(\overrightarrow{f}_j^Q)^{\text{visc}}\Big).$$

A sufficient condition to get the momentum conservation property is then [11]

$$\sum_{j,j\in Q}(\overrightarrow{f}_j^Q)^{\text{visc}}=0. \tag{4.15}$$

Before we explain how this condition is imposed, we show that the total energy is conserved in semi-discrete form. The total energy balance for the entire domain is

$$\begin{aligned}\frac{\mathrm{d}}{\mathrm{d}t}\Big(\sum_Q m_Q\epsilon_Q+\sum_j\frac{m_j\overrightarrow{u}_j^2}{2}\Big)&=\sum_Q m_Q\frac{\mathrm{d}\epsilon_Q}{\mathrm{d}t}+\sum_j m_j\overrightarrow{u}_j\cdot\frac{\mathrm{d}\overrightarrow{u}_j}{\mathrm{d}t}\\&=\sum_Q\Big(-\sum_{j,j\in Q}\overrightarrow{u}_j\cdot(\overrightarrow{f}_j^Q)\Big)+\sum_j\overrightarrow{u}_j\cdot\Big(\sum_{Q,Q\ni j}(\overrightarrow{f}_j^Q)\Big),\end{aligned} \tag{4.16}$$

where

$$(\overrightarrow{f}_j^Q)=(\overrightarrow{f}_j^Q)^{\text{pres}}+(\overrightarrow{f}_j^Q)^{\text{visc}}. \tag{4.17}$$

By interchanging the order of the double sum, one trivially check that total energy is conserved. Thus, the scheme is conservative in its semi-discretized form if the condition (4.15) is satisfied.

Second, we want the scheme to satisfy an entropy inequality. Actually, the introduction of artificial viscosity into the scheme modifies the time rate of entropy on cell Q:

$$\begin{aligned}m_QT_Q\frac{\mathrm{d}S_Q}{\mathrm{d}t}&=-\sum_{j,j\in Q}(\overrightarrow{f}_j^Q)^{\text{visc}}\cdot\overrightarrow{u}_j=\sum_{j,j\in Q}(\overrightarrow{f}_j^Q)^{\text{visc}}\cdot(\overrightarrow{u}^\star_Q-\overrightarrow{u}_j)-\sum_{j,j\in Q}(\overrightarrow{f}_j^Q)^{\text{visc}}\cdot\overrightarrow{u}^\star_Q\\&=\sum_{j,j\in Q}[\mathcal{M}_j^Q(\overrightarrow{u}^\star_Q-\overrightarrow{u}_j)]\cdot(\overrightarrow{u}^\star_Q-\overrightarrow{u}_j)-\Big(\sum_{j,j\in Q}(\overrightarrow{f}_j^Q)^{\text{visc}}\Big)\cdot\overrightarrow{u}^\star_Q.\end{aligned}$$

The matrix $\mathcal{M}_j^Q$ is a 2×2 symmetric positive definite matrix, then the first term on the right hand side is positive. The second term is zero if condition (4.15) is satisfied.

We derived a single condition which is sufficient to get a conservative and entropic scheme. Now, since this condition is not satisfied, we have to do something to force the viscous force to satisfy it. Our idea is to make use of the fact that the degrees of

freedom $\{\overrightarrow{u}^{\star}_{Q}\}$ are still unknown. The condition (4.15) can be rewritten using the matrix formalism

$$\sum_{j,j\in Q}\mathcal{M}^{Q}_{j}\left(\overrightarrow{u}^{\star}_{Q}-\overrightarrow{u}_{j}\right)=0. \tag{4.18}$$

This can be interpreted as a non-linear problem with $\overrightarrow{u}^{\star}_{Q}$ as unknown. Then, the cell approximate velocity is defined by

$$\overrightarrow{u}^{\star}_{Q}=\Big[\sum_{j,j\in Q}\mathcal{M}^{Q}_{j}\Big]^{-1}\sum_{j,j\in Q}\left(\mathcal{M}^{Q}_{j}\overrightarrow{u}_{j}\right). \tag{4.19}$$

The system (4.19) is non linear. It can be solved utilizing an iterative algorithm (we get satisfaction with a fixed point method).

To end this section, it is interesting to notice that the half Riemann problems introduce the necessary coupling between the extra degree of freedom $\{\overrightarrow{u}^{\star}_{Q}\}$ and the nodes velocity $\{\overrightarrow{u}_{j}\}$. It is surprising to state that the solution (4.19) can actually be interpreted as a cell velocity approximation. To be convinced of that, one could express the exact solution of system (4.18) for some particular trivial cases. It appears that $\overrightarrow{u}^{\star}_{Q}$ is a balance average of the cell node velocities.

4.2 Limiter function

The viscous force previously described is active even in the case of isentropic flows, which results in an extra entropy production. Following [3], a limiter function is introduced to eliminate linear velocity fields. This section is devoted to the presentation of its construction.

The viscous force acting on node j from cell Q is the sum of two forces:

$$\begin{aligned}\left(\overrightarrow{f}^{Q}_{j}\right)^{\text{visc}}&=\mathcal{M}^{Q}_{\frac{1}{2}e(j-1/2,j)}\left(\overrightarrow{u}^{\star}_{Q}-\overrightarrow{u}_{j}\right)+\mathcal{M}^{Q}_{\frac{1}{2}e(j,j+1/2)}\left(\overrightarrow{u}^{\star}_{Q}-\overrightarrow{u}_{j}\right)\\&=\overrightarrow{f}^{Q}_{\frac{1}{2}e(j-1/2,j)}+\overrightarrow{f}^{Q}_{\frac{1}{2}e(j,j+1/2)}.\end{aligned} \tag{4.20}$$

For each half-edge (for example $[M_j,M_{j+1/2}]$) containing the node j, we compute a function

$$\varphi^{Q}_{\frac{1}{2}e(j,j+1/2)}\in[0,1],$$

which turns the force

$$\left(\overrightarrow{f}^{Q}_{\frac{1}{2}e(j,j+1/2)}\right)^{\text{visc}},$$

off for situations in which the velocity difference with respect to the normal direction $\overrightarrow{n}^{Q}_{\frac{1}{2}e(j,j+1/2)}$ is a linear function of the local coordinates. This limiter function is described in [3].

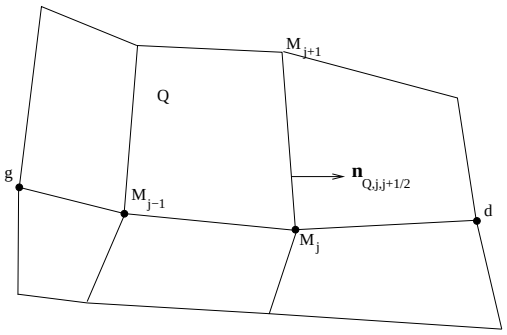

Figure 4: Notations for the limiter function.

We introduce the nodes g and d which are the nearest neighbors to the end points j and $j-1$ (Fig. 4). We define

$$S_d = \frac{(\overrightarrow{u}_d - \overrightarrow{u}_j)\cdot \overrightarrow{n}^Q_{\frac{1}{2}e(j,j+1/2)}}{(\overrightarrow{x}_d - \overrightarrow{x}_j)\cdot \overrightarrow{n}^Q_{\frac{1}{2}e(j,j+1/2)}} \Bigg/ \frac{(\overrightarrow{u}_j - \overrightarrow{u}_{j-1})\cdot \overrightarrow{n}^Q_{\frac{1}{2}e(j,j+1/2)}}{(\overrightarrow{x}_j - \overrightarrow{x}_{j-1})\cdot \overrightarrow{n}^Q_{\frac{1}{2}e(j,j+1/2)}}, \tag{4.21}$$

$$S_g = \frac{(\overrightarrow{u}_{j-1} - \overrightarrow{u}_g)\cdot \overrightarrow{n}^Q_{\frac{1}{2}e(j,j+1/2)}}{(\overrightarrow{x}_{j-1} - \overrightarrow{x}_g)\cdot \overrightarrow{n}^Q_{\frac{1}{2}e(j,j+1/2)}} \Bigg/ \frac{(\overrightarrow{u}_j - \overrightarrow{u}_{j-1})\cdot \overrightarrow{n}^Q_{\frac{1}{2}e(j,j+1/2)}}{(\overrightarrow{x}_j - \overrightarrow{x}_{j-1})\cdot \overrightarrow{n}^Q_{\frac{1}{2}e(j,j+1/2)}}. \tag{4.22}$$

The limiter function is defined by

$$\varphi^Q_{\frac{1}{2}e(j,j+1/2)} = \max\Big\{0, \min\Big\{\frac{S_d+S_g}{2}, 2S_d, 2S_g, 1\Big\}\Big\}. \tag{4.23}$$

At the end, the viscous force $\overrightarrow{f}^Q_{\frac{1}{2}e(j,j+1/2)}$ is replaced by

$$\Big(1-\varphi^Q_{\frac{1}{2}e(j,j+1/2)}\Big)\overrightarrow{f}^Q_{\frac{1}{2}e(j,j+1/2)}.$$

The entropy inequality is still valid in the presence of the limiter function. Another interesting point is that with the limiter function, the viscous force has no effects along a constant wave front. The weak point in such an approach is that a shock direction approximation is implicitly introduced by construction.

The role of the limiter function can be interpreted in a quiet different way. It can be viewed as "a sort of" second order accurate reconstruction of the velocity field in specific directions, or like a modification of the velocity gradients which are reduced by the limiter function in the regions where the flow is smooth.

4.3 Compression criterion

There is a major difference between non conservative schemes based on the introduction of an artificial term and Godunov type ones. In the first approach (and contrary to the second one), it is common practice to maintain the viscosity term only in compression and

to set it to zero everywhere else. Indeed, rarefactions in gases usually do not need viscosity. A switch term is introduced in the method to determine compression and expansion (typically based on the sign of the velocity divergence on the cell or the compression of each individual edge). Therefore, the artificial viscous force does not vary continuously. This can produce numerical instabilities. As the positivity of the performed work is usually ensured with the test used to determine whether a cell is in compression or not, there is not any other possible choice.

Our form of artificial viscosity is dissipative independently of any compression criteria. In practice, the viscous force is computed at each time iteration (with the limiter function) and it is systematically taken into account in the equations.

4.4 Time discretization

A central difference method is used for time discretization. The velocity is staggered in time with respect to the displacement to get an explicit second order accurate integration rule [20]. We define

$$\Delta t^n = t^{n+1} - t^n.$$

We compute

$$\overrightarrow{u}_j^{n+\frac{1}{2}} = \overrightarrow{u}_j^{n-\frac{1}{2}} + \left(\overrightarrow{f}_j^n / m_j\right)\Delta t^n,$$
$$\overrightarrow{x}_j^{n+1} = \overrightarrow{x}_j^n + \overrightarrow{u}_j^{n+\frac{1}{2}}\Delta t^{n+\frac{1}{2}},$$

with

$$\Delta t^{n+\frac{1}{2}} = \frac{1}{2}\left(\Delta t^n + \Delta t^{n+1}\right).$$

Thermodynamics variables (density and internal energy) are computed at time t^n.

Two time step limitations are used. The first one is a CFL like criterion. We define

$$\Delta t_{cfl}^n = C_{cfl} \min_Q \left(\frac{L_Q^n}{a_Q^n}\right),$$

where L_Q^n is the minimal value of the distance between two points of the cell and C_{cfl} is a positive constant. The value $C_{cfl} = 0.3$ provides stable results.

For the second criterion, based on the variation of the volume, we compute

$$\Delta t_\rho^n = \frac{\Delta t^{n-1}}{\max_Q \left(\frac{(\Delta\rho)_Q}{\rho_Q^n}\right)},$$

where $\Delta\rho$ is the density growth over the previous time iteration.

At the end,

$$\Delta t^n = \min\left\{\Delta t_{cfl}^n, \Delta t_\rho^n\right\}.$$

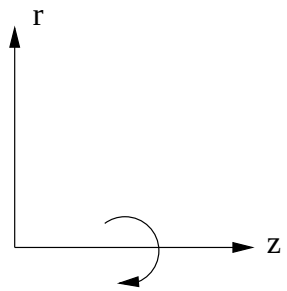

Figure 5: Cylindrical coordinates with rotational symmetry about the z-axis.

4.5 Cylindrical geometry

Some problems with axisymmetrical geometry are presented in this paper. In this section, we explain how we proceed. We denote by (r,z) the cylindrical coordinates with rotational symmetry about the z-axis (see Fig. 5).

The formulations are written in terms of (r,z) coordinates by introducing the elemental volume $r\mathrm{d}r\mathrm{d}z$ in place of $\mathrm{d}x\mathrm{d}y$. We want the scheme to preserve spherical symmetry for equal angle zoning.

Following Caramana and Whalen [22], we use the area-weighted discretization. In the equation for momentum, the pressure gradient is approximated by

$$\int_{\mathcal{C}_j} \overrightarrow{\nabla} P \; r\mathrm{d}r\mathrm{d}z \simeq r_j \int_{\mathcal{C}_j} \overrightarrow{\nabla} P \; \mathrm{d}r\mathrm{d}z. \tag{4.24}$$

The cartesian node mass is denoted by m_j^c and

$$m_j = \int_{\mathcal{C}_j} \rho \; r\mathrm{d}r\mathrm{d}z \simeq r_j \sum_{Q, Q \ni j} \rho_Q \int_{Q \cap \mathcal{C}_j} \mathrm{d}r\mathrm{d}z = r_j m_j^c. \tag{4.25}$$

At the end, it comes to integrate the equation for momentum in cartesian coordinates

$$m_j^c \frac{\mathrm{d}\,\overrightarrow{u}_j}{\mathrm{d}t} + \sum_{Q, Q \ni j} \int_{(\partial \mathcal{C}_j) \cap Q} P \overrightarrow{n} \, \mathrm{d}S = 0. \tag{4.26}$$

The internal energy equation (3.8) is now modified to take into account the work done by the viscous force:

$$m_Q \frac{\mathrm{d}\epsilon_Q}{\mathrm{d}t} + P_Q \frac{\mathrm{d}V_Q(t)}{\mathrm{d}t} = -\sum_{j, j \in Q} \left(\overrightarrow{f}_j^{\,Q}\right)^{\mathrm{visc}} \cdot \left(r\overrightarrow{u}\right)_j \simeq -r_Q \sum_{j, j \in Q} \left(\overrightarrow{f}_j^{\,Q}\right)^{\mathrm{visc}} \cdot \overrightarrow{u}_j, \tag{4.27}$$

where r_Q is a mean value of r on element Q. In the present study, r_Q is the r coordinate of the center point of the element. Total energy is not conserved by this scheme. In [4], compatible Area-weighted schemes are proposed.

There is no specific treatment for the computation of the viscous force in the case of cylindrical geometry.

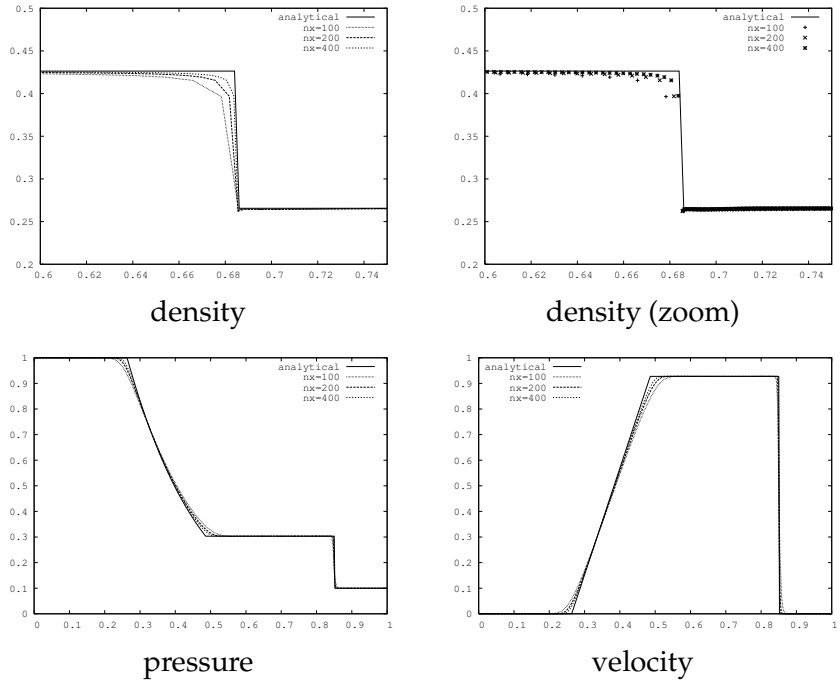

Figure 6: Sod's shock tube problem.

5 Numerical experiments

All the numerical experiments presented in the following section are performed without any Hourglass stabilization [19]. The viscous force is computed all the time, for compressions as well as expansions.

5.1 Sod's shock tube problem

We consider first a one-dimensional shock tube problem, to test the capability of the method to handle solutions with discontinuities. At initial time, the left state is $\rho_L=1$, $P_L=1$, $u_L=1$, the right state is $\rho_R=0.125$, $P_R=0.1$ and $u_R=0$. The computational domain is defined by $(x,y)\in[0,1]\times[0,0.1]$. The interface is located at $x=0.5$. The initial mesh is a Cartesian grid with $n_x\times 2$ equally spaced cells. We impose wall boundary conditions at each boundary. The results obtained with $n_x=100$, $n_x=200$ and $n_x=400$ are presented in Fig. 6. Almost converged solutions are provided with $n_x=400$.

5.2 Saltzman problem

This well-known problem consists in solving a one-dimensional problem on a slightly non-uniform mesh [18]. The computational domain is defined by $(x,y)\in[0,1]\times[0,0.1]$.

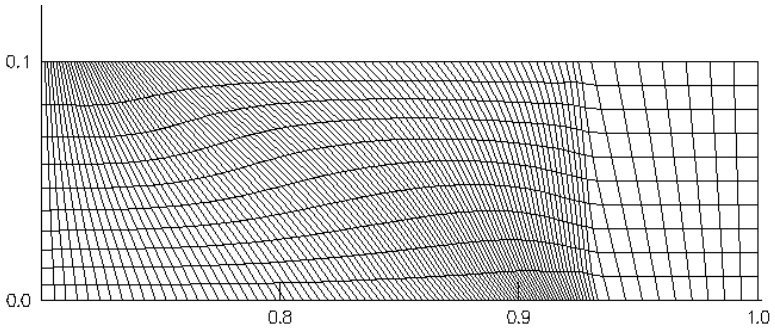

Figure 7: Saltzman problem. Mesh at time $t=0.7$.

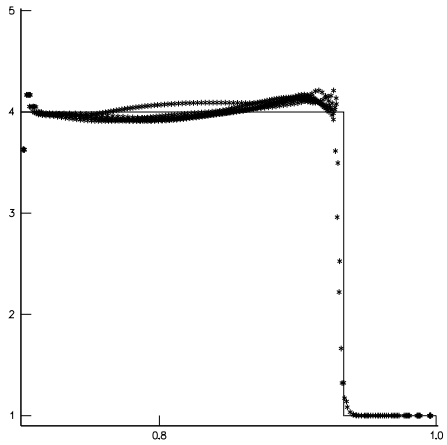

Figure 8: Saltzman problem. Density as a function of the position at time $t=0.7$. Exact solution (solid lines) and approximate solution ($\star$).

The left end of the box is a piston, which moves into the box with a constant velocity of 1.0.

The initial mesh is composed of 100×10 non uniform cells defined as

$$x(i,j)=i\Delta x+(10-j)\Delta y\sin(0.01\pi i),$$
$$y(i,j)=j\Delta y,$$

where

$$\Delta x=\Delta y=0.01.$$

At initial time, the box is filled with a perfect gas ($\gamma=5/3$) of unit density and very low internal energy ($\epsilon=10^{-6}$). Fig. 8 shows the density on each element as a function of the position of the cell gravity center. The one-dimensional symmetry is well preserved. Considering that no Hourglassing treatment is used, the quality of the resulting mesh at time $t=0.7$ is good (Fig. 7). The resulting mesh at a latter time ($t=0.9$) shows some

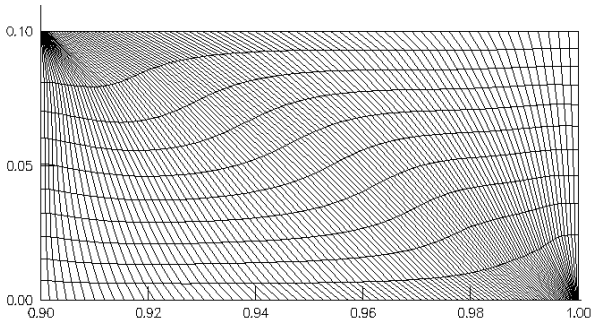

Figure 9: Saltzman problem. Mesh at time $t=0.9$.

accumulations of grid points along the boundary axis (Fig. 9). We suspect a problem of boundary conditions due to the staggered placement of variables.

5.3 Noh test

This test is detailed in [16]. The initial state of the fluid is uniform. The velocity has a radial distribution (the velocity points to the origin and has unit magnitude, except at the origin, where it is forced to zero). The density and pressure are $\rho^0=1$ and $P^0=0$. For practical purposes, the initial pressure $P^0=10^{-10}$ is used. The fluid is an ideal gas with $\gamma=5/3$. A shock wave is generated at the origin and propagates radially outward.

5.3.1 Polar grid

We first test the Noh problem in a cylindrical coordinates system, using a polar grid with same angular zoning. The initial computational domain is defined by $(r,\theta)\in[0,1]\times[0,\theta_{\max}]$. The initial mesh is composed by $n_r\times n_\theta$ equally spaced cells. We take $n_\theta=2$. The peak post shock density should be $\rho=64$. Results are displayed for two meshes with $n_r=50$ and $\theta_{\max}=2$ or $\theta_{\max}=4$ (Fig. 10). The wave front invariance property is well satisfied. Results are shown for different radial zonings (Fig. 11). The method converges to the correct solution.

An ultimate simulation is proposed to show the scheme actually preserves the spherical symmetric property. It is performed on the region $(r,\theta)\in[0,1]\times[0,90]$ with $n_\theta=90$ and $n_r=100$ (see Figs. 12 and 13).

5.3.2 Cartesian grid

We test the Noh problem in a Cartesian coordinates system, using a Cartesian grid. The initial computational domain is defined as $(x,y)\in[0,1]\times[0,1]$. In this case, the peak post density is $\rho=16$. The numerical results obtained with an edge-centered viscosity [3] exhibit unphysical vorticity along boundary axes (Fig. 14). The solution obtained with the proposed node-centered viscosity is good (see Fig. 15), especially on the axes. But the solution of Campbell and Shashkov [13] is still better.

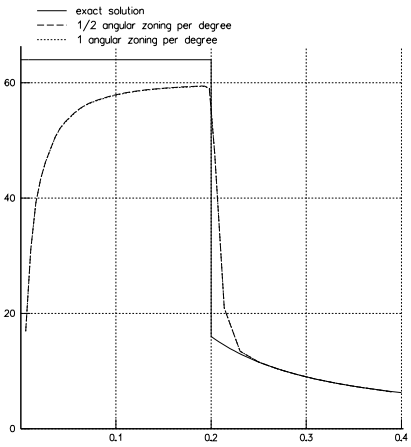

Figure 10: Noh problem. Spherical geometry. Density profiles at time 0.6 for two different angular zonings ($(r,\theta)\in[0,1]\times[0,2]$ and $(r,\theta)\in[0,1]\times[0,4]$ with $n_\theta=2$), same radial zoning ($n_r=50$). Comparison with analytical solution.

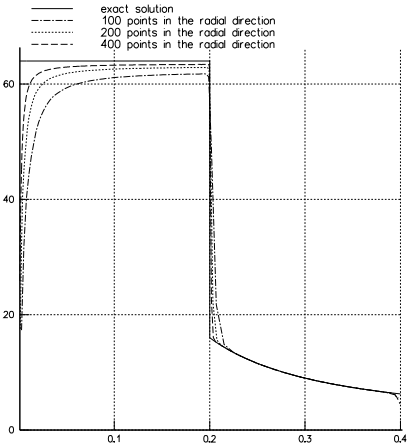

Figure 11: Noh problem. Spherical geometry. Domain $(r,\theta)\in[0,1]\times[0,4]$. Density profiles at time 0.6 for different radial zonings ($n_r=100$, $n_r=200$ and $n_r=400$), same angular zoning (1/2 angular zoning per degree). Comparison with analytical solution.

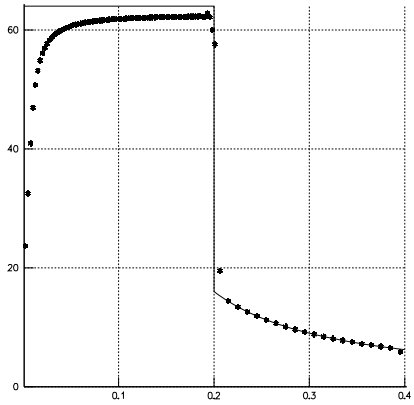

Figure 12: Noh problem. Spherical geometry. Domain $(r,\theta)\in[0,1]\times[0,90]$, $n_r=100$, $n_\theta=90$. Density as function of the position for all the mesh nodes. Comparison with analytical solution.

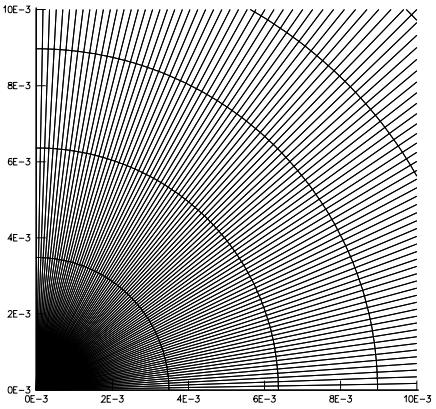

Figure 13: Noh problem. Spherical geometry. Domain $(r,\theta)\in[0,1]\times[0,90]$, $n_r=100$, $n_\theta=90$. Mesh (zoom) at time 0.6.

5.4 The Sedov blast wave problem

We consider the Sedov explosion test problem in cylindrical symmetry. It models the expanding wave by an intense explosion in a perfect gas. The problem consists of an ideal gas ($\gamma=1.4$) with a delta-function energy source at the origin. The computational domain is defined as $(x,y)\in[0,1.2]\times[0,1.2]$. The initial conditions are $\rho_0=1$, $P_0=10^{-6}$ and $\overrightarrow{u}_0=0$. The energy source at the origin is deposited in a volume V_0 (which is the

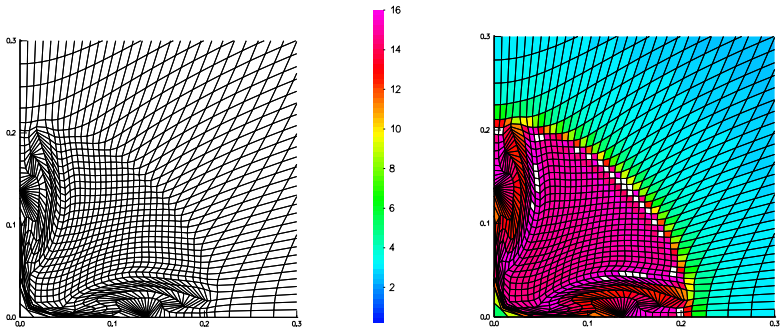

Figure 14: Noh problem. Cartesian geometry. Results obtained with an edge-centered viscosity. Mesh and density at time 0.6.

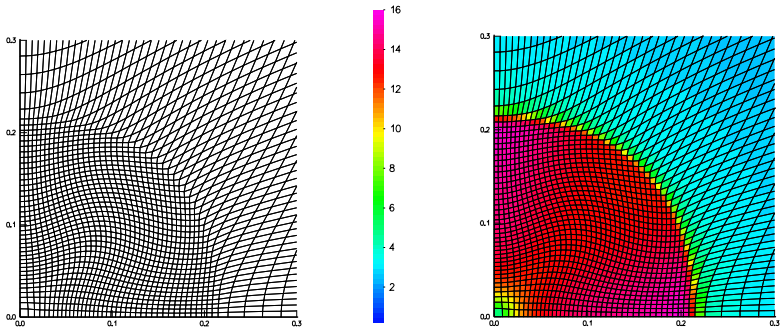

Figure 15: Noh problem. Cartesian geometry. Results obtained with the proposed node-centered viscosity. Mesh and density at time 0.6.

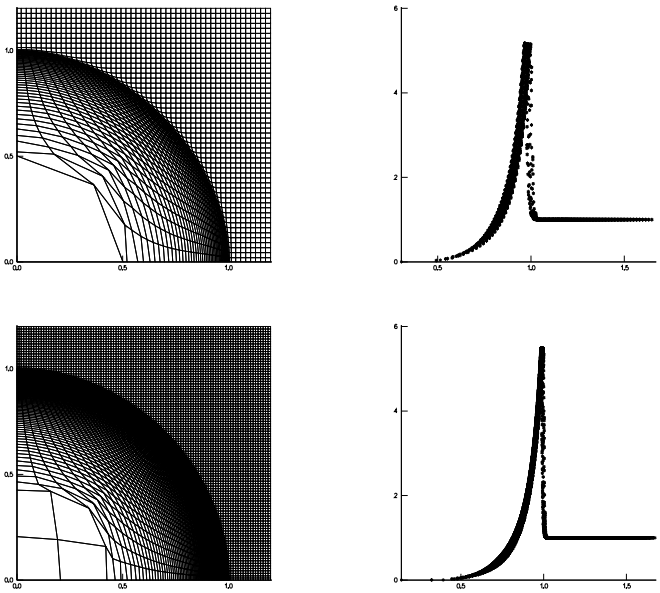

Figure 16: The Sedov blast wave problem. Cartesian meshes. Top: 51×51 elements. Bottom: 102×102 elements. Mesh and density as function of the position (for all the mesh nodes) at time 1.

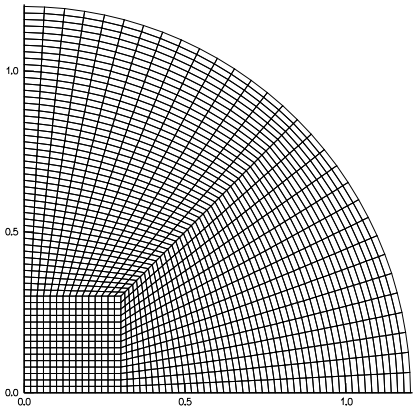

Figure 17: The Sedov blast wave problem. Initial unstructured mesh.

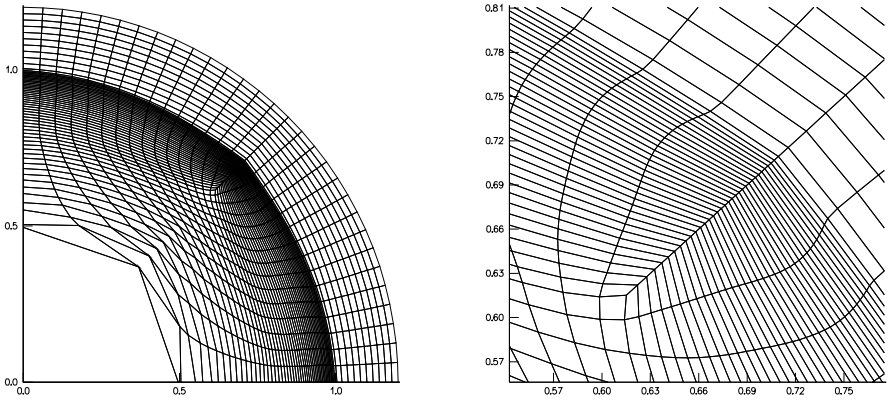

Figure 18: The Sedov blast wave problem. Unstructured mesh.

same for all the meshes) such as $(\rho_0 V_0 \epsilon_0) = 0.244816$. The solution is a diverging shock whose front is located at radius 1 at time $t = 1$. The value of the peak density is 6. Results with different meshes are proposed. First, we consider two Cartesian grids composed by 51×51 and 102×102 elements. The results are shown in Fig. 16. The one-dimensional symmetry of the solution is well preserved. The shock position is in agreement with the theory. The solution converges to the correct value of the peak density. Then, we consider the same problem on an unstructured grid displayed in Fig. 17. The initial grid quality is intentionally bad (no smoothing). The same grid has been considered by Maire [11] who obtained very good results with its high-order cell-centered Lagrangian scheme. The quality of the mesh at $t = 1$ is good in the vicinity of the triple point (Fig. 18). We think this is due to the absence of a compressive test in the proposed artificial viscosity.

6 Conclusions

In this paper, we propose a new artificial viscosity for Lagrangian schemes based on a staggered placement of variables. This work is motivated by [10, 14].

The method is defined by introducing a cell-centered approximation for the velocity. The Riemann problem can be defined in a very natural way, by proceeding exactly like in the case of a cell-centered finite volume scheme. The method is based on the double shock approximate solver, like all other existing artificial viscosities. In our past experience, the numerical solutions obtained with the node-centered viscosity exhibit very few Hourglass-type deformations. The numerical results exhibit good stability and accuracy properties.

In the future, we intend to improve the solver by deriving a second-order extension of the method. An higher-order reconstruction of the velocity gradients would result in a production of entropy better adapted to the problem to be solved. The objective is also to get a fully multidimensional method for the treatment of shock waves. Of course, this would be an alternative to the limiter function which drawback is that it introduces a shock direction approximation.

Acknowledgments

I thank Bernard Rebourcet for his encouragement and constructive suggestions. I am also grateful to Pierre-Henri Maire, Céline Baranger and Sophie Borel-Sandou who read the evolving manuscript and shaped the final version through their insightful comments.

References

[1] J. Von Neumann and R. D. Richtmyer, A method for the numerical calculation of hydrodynamics shocks, J. Comput. Phys., 21 (1950), 232–237.
[2] W. D. Schulz, Tensor artificial viscosity for numerical hydrodynamics, J. Math. Phys., 5 (1964), 133–138.
[3] E. J. Caramana, M. J. Shashkov and P. P. Whalen, Formulations of artificial viscosity for multi-dimensional shock wave computations, J. Comput. Phys., 144 (1998), 70–97.
[4] E. J. Caramana, D. E. Burton, M. J. Shashkov and P. P. Whalen, The construction of compatible hydrodynamics algorithms utilizing conservation of total energy, J. Comput. Phys., 146 (1998), 227–262.
[5] J. K. Dukowicz, A general, non-iterative Riemann solver for Godunov's method, J. Comput. Phys., 61 (1985), 119–137.
[6] R. B. Christensen, Godunov methods on a staggered mesh–an improved artificial viscosity, Technical Report UCRL-JC 105269, LLNL (1990).
[7] S. Godunov et coll., Résolution Numérique des Problèmes Multidimensionnels de la Dynamique des Gaz, Editions MIR, Moscou (1979).
[8] M. L. Wilkins, Calculation of elastic plastic flow, Methods in Computational Physics, Academic Press, New York, 3 (1964).

[9] M. L. Wilkins, Computer Simulation of Dynamic Phenomena, Scientific Computation, Springer, (1999).
[10] P.-H. Maire, R. Abgrall, J. Breil and J. Ovadia, A cell-centered Lagrangian scheme for two-dimensional compressible flow problems, SIAM. J. Sci. Comput., 29 (4) (2007), 1781–1824.
[11] P.-H. Maire, A high-order cell-centered Lagrangian scheme for two-dimensional compressible fluid flows on unstructured meshes, J. Comput. Phys., 228 (2009), 2391–2425.
[12] P.-H. Maire, A high-order cell-centered Lagrangian scheme for compressible fluid flows in two-dimensional cylindrical geometry, J. Comput. Phys., 228 (2009), 6882–6915.
[13] J. C. Campbell and M. J. Shashkov, A tensor artificial viscosity using a mimetic finite difference algorithm, J. Comput. Phys., 172 (4) (2001), 739–765.
[14] B. Després and C. Mazeran, Lagrangian gas dynamics in two dimensions and Lagrangian systems, Arch. Ration. Mech. An., 178 (2005), 327–372.
[15] R. Landshoff, A numerical method for treating fluid flow in the presence of shocks, Technical Report LA-1930, Los Alamos National Laboratory, (1955).
[16] W. F. Noh, Errors for calculations of strong shocks using artificial viscosity and an artificial heat flux, J. Comput. Phys., 72 (1987), 78–120.
[17] G. A. Sod, A survey of several finite difference methods for systems of non-linear hyperbolic conservation laws, J. Comput. Phys., 27 (1078), 1–31.
[18] J. K. Dukowicz and B. J. A. Meltz, Vorticity errors in multidimensional Lagrangian codes, J. Comput. Phys., 99 (1992), 115–134.
[19] D. P. Flanagan and T. Belytschko, A uniform strain hexaedron and quadrilatera with orthogonal hourglass control, Int. J. Numer. Meth. Eng., 17 (1982), 679–706.
[20] D. J. Benson, Computational methods in Lagrangian and Eulerian hydrocodes, Comput. Method. Appl. M., 99 (1992), 235–394.
[21] E. J. Caramana and M. J. Shashkov, Elimination of artificial grid distortion and Hourglass-type motions by means of Lagrangian Subzonal masses and pressures, J. Comput. Phys., 142 (1998), 521–561.
[22] E. J. Caramana and P. P. Whalen, Numerical preservation of symmetry p roperties of continuum problems, J. Comput. Phys., 141 (1998), 174–198.
[23] P. P. Whalen, Algebraic limitations on two-dimensional hydrodynamics simulations, J. Comput. Phys., 124 (1996), 46–54.